

# Brachistochrone curve of a fluid filled cylinder: Not too fast, not too slow

Srikanth Sarma Gurram<sup>1</sup>, Sharan Raja<sup>1</sup>, Mahesh V. Panchagnula<sup>2†</sup>  
and Pallab Sinha Mahapatra<sup>1</sup>

<sup>1</sup>Department of Mechanical Engineering, Indian Institute of Technology Madras, Chennai  
600036 India,

<sup>2</sup>Department of Applied Mechanics, Indian Institute of Technology Madras, Chennai 600036  
India

(Received xx; revised xx; accepted xx)

The brachistochrone curve for a non-dissipative particle tries to maximize inertia of the particle but for a fluid filled cylinder, increasing inertia would amount to increased dissipative losses. Hence the trade-off between inertia and dissipation plays a vital role in determining the brachistochrone curve of a fluid filled cylinder. This trade-off manifests itself in the form of an integro-differential equation governing the angular acceleration of the cylinder. Here, we compute the brachistochrone curve of a fluid filled cylinder using optimal control principles and investigate the effect of the aforementioned trade-off on the deviation of the brachistochrone curve from that of a non-dissipative particle. Also, we investigate the effects of the non-dimensional parameters of the problem on the shape of the brachistochrone curve. We then analyze the stability of the time varying fluid flow in the cylinder and find an admissible region for the terminal point which would ensure the stability of the fluid flow as the cylinder rolls along the brachistochrone curve.

**Key words:** Optimal control, Dissipative dynamics, Brachistochrone, Stability of time dependent flows

## 1. Introduction

The problem of brachistochrone curve has been of interest since Bernoulli posed it as a challenge in [Andre-Sohn \(1696\)](#). This problem was the inception of calculus of variations and thereby led to optimal control. Most literature in optimal control deals with systems with state equations where the velocities at the current moment will be a function of only the current position and the current control action i.e., the time evolution of the system can be determined by just the current state and the future control actions. In the case of a fluid filled cylinder, the combined time evolution of the fluid and the cylinder can be determined if the current velocity information of the cylinder, the velocity field of the fluid flow and the future control actions are given. But, computing the flow field at each time step can become computationally intensive. By removing the velocity field of the fluid from explicitly appearing in the state equation of the cylinder, we end up with an equation which would need all of the past values of the cylinder velocities to compute the time evolution. This memory dependence of the system is what makes the fluid filled cylinder interesting. This property has been illustrated in [Supekar & Panchagnula](#)

† Email address for correspondence: mvp@iitm.ac.in

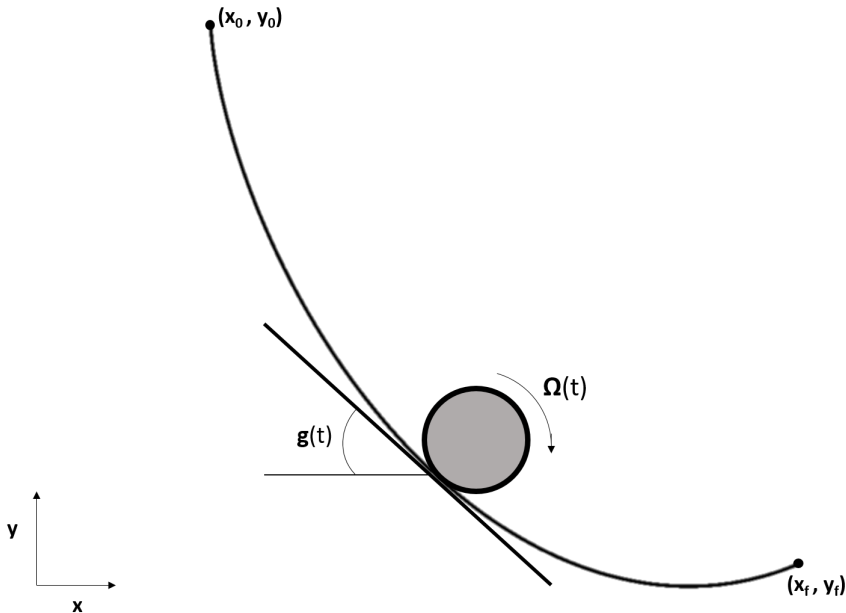


FIGURE 1. Schematic of the problem statement

(2014) while discussing the dynamics of a fluid filled cylinder rolling down an inclined plane.

Over years, the brachistochrone problem has been extended by many people like Gemmer *et al.* (2006) by introducing field varying gravity, Lipp (1997) by including coulomb friction and Vratanaar & Saje (1998) by including non-conservative forces. Despite a long history of the brachistochrone problem, it has not been extended into fluid mechanics context except by modeling fluid effects empirically as done by Lipp (1997). Our work tries to close this gap in the literature by using the coupled equations of fluid mechanics and rigid body mechanics to find the brachistochrone curve of a fluid filled cylinder. The obtained curve can find applications in transporting liquid drops on a super hydrophobic surface in the fastest time.

Intuition says that for both high viscosity and low viscosity limits of the fluid, we retrieve back cycloid as a brachistochrone curve. So, by Rolle's theorem, there must exist a viscosity value at which the deviation from cycloid is maximum. To quantify this, we define two metrics for the deviation from a cycloid, one being a geometric deviation and the other a kinematic deviation.

The question we would be answering in this paper is as follows:

*“Given two points A and B in a vertical plane, what is the curve traced out by the center of mass of a fluid filled cylinder acted only by gravity, who's center of mass starts at A and reaches B in the shortest time?”*

## 2. Problem formulation

The equations governing a fluid filled cylinder are the rigid body equations for the cylindrical shell, Navier Stokes for the fluid and boundary conditions coupling both these

equations. In the following section, we derive the governing equations for the case of a fluid filled cylinder rolling down an arbitrary curve in x-y plane.

### 2.1. Governing equations

The Navier stokes equations for the fluid flow in the rotating frame of reference of the rolling cylinder are as follows:

$$-\frac{v^2}{r} = \dot{\Omega}R \cos(\theta - \gamma(t)) - g \sin(\theta) - \frac{\partial p}{\partial r} \quad (2.1a)$$

$$\frac{\partial v}{\partial t} = -\dot{\Omega}R \sin(\theta - \gamma(t)) - g \cos(\theta) - \frac{1}{r} \frac{\partial p}{\partial \theta} + \nu \frac{\partial}{\partial r} \left( \frac{1}{r} \frac{\partial}{\partial r} (rv) \right) \quad (2.1b)$$

Where,  $v$  is the azimuthal velocity with respect to the center of mass of the cylindrical shell,  $\gamma(t)$  is the inclination of the curved incline written in Lagrangian framework,  $\Omega(t)$  is the instantaneous angular velocity of the cylinder,  $g$  is the acceleration due to gravity,  $r$  and  $\theta$  are the normal polar coordinates. We can break down the pressure field  $p(r, \theta, t)$  as

$$p(r, \theta, t) = (\dot{\Omega}R \cos(\theta - \gamma(t)) - g \sin(\theta))r + p_d(r, t) \quad (2.2)$$

Substituting the above form of the pressure field will lead us to the following equation:

$$\frac{\partial v}{\partial t} = \nu \frac{\partial}{\partial r} \left( \frac{1}{r} \frac{\partial}{\partial r} (rv) \right) \quad (2.3)$$

The boundary conditions being:

$$v(R, t) = R\Omega(t) \quad (2.4a)$$

$$\frac{\partial v}{\partial r}(0, t) = 0 \quad (2.4b)$$

The rigid body equations for the cylinder are:

$$(m + M)R\dot{\Omega} = (m + M)g \sin \gamma(t) - f \quad (2.5a)$$

$$MR^2\dot{\Omega} = fR - T \quad (2.5b)$$

$$T(t) = 2\pi\mu R^2 h \left( \frac{\partial v}{\partial r} - \frac{v}{r} \right) \Big|_{r=R} \quad (2.6)$$

The cylinder would be starting from rest and the fluid would be quiescent. So,

$$\Omega(0) = 0 \quad \text{and} \quad v(0, r) = 0 \quad (2.7)$$

Now, we must look for a solution for the equations 2.3 to 2.7. [Batchelor \(2000\)](#) presents a closed form solution for Equation 2.3 with a constant boundary condition. But, here we have a time dependent boundary condition whose evolution is governed by the rigid body equations 2.5. [Supekar & Panchagnula \(2014\)](#) have extended the closed form solution of [Batchelor \(2000\)](#) to the case of a time varying boundary condition using duhammel's theorem and thereby, a solution was obtained for the case of a cylinder rolling down an inclined plane. We extend the same solution for our case by arguing that any curve in the x-y space is nothing but an inclined plane with it's inclination varying with space (or time in a Lagrangian framework). Using this solution, we can eliminate the equation 2.3 and be left with only equations 2.5 and 2.6. These equations lead to the following:

$$v(r, t) = \int_{\tau=0}^t \left( r + 2R \sum_{n=1}^{\infty} \frac{J_1\left(\lambda_n \frac{r}{R}\right)}{\lambda_n J_0(\lambda_n)} \exp\left(-\lambda_n^2 \frac{\nu(t-\tau)}{R^2}\right) \right) \dot{\Omega}(\tau) d\tau \quad (2.8)$$

$$(m + 2M)R^2 \dot{\Omega}(t) = -T(t) + (m + M)gR \sin(\gamma(t)) \quad (2.9a)$$

$$T(t) = \sum_{n=1}^{\infty} \int_{\tau=0}^t \exp(-\lambda_n^2(t-\tau)) \dot{\Omega}(\tau) d\tau \quad (2.9b)$$

Where  $\lambda_n$  is the  $n^{th}$  root of the Bessel function of first kind. Now, we non-dimensionalize the above equations with  $\frac{R^2}{\nu}$  as the time scale,  $R$  as the length scale and  $\rho\pi R^2 h$  as the mass scale. As a result of this, we obtain two non-dimensional parameters:  $\pi_m = \frac{M}{\rho R^2 h}$  and  $\pi_g = \frac{gR^3}{\nu^2}$ . The resulting non-dimensional equations are:

$$(1 + 2\pi_m)\dot{\Omega}(t) = -4g(t) + (1 + \pi_m)\pi_g \sin(\gamma(t)) \quad (2.10)$$

where,

$$g(t) = \sum_{n=1}^{\infty} \int_{\tau=0}^t \exp(-\lambda_n^2(t-\tau)) \dot{\Omega}(\tau) d\tau \quad (2.11)$$

## 2.2. Optimization problem

We now formulate an optimization problem in the optimal control framework presented in [Liberzon \(2011\)](#). In this framework, the position  $(x(t), y(t))$  and angular velocity  $\Omega(t)$  of the cylinder comprise the state space of the cylinder and the inclination of the curve  $\gamma(t)$  will be the control action which controls the trajectory of the cylinder. Now, the problem is to find the control action  $\gamma(t)$  which will minimize the time of descent of the cylinder from a point A to point B. The kinematic equations of motion of the cylinder are:

$$\dot{x}(t) = \Omega(t) \cos(\gamma(t)) \quad (2.12)$$

$$\dot{y}(t) = -\Omega(t) \sin(\gamma(t)) \quad (2.13)$$

The optimization problem is now formulated as:

$$\underset{\gamma(t) \in [-\frac{\pi}{2}, \frac{\pi}{2}]}{\text{Minimize}} J(\gamma(t)) = \int_0^T dt \quad (2.14)$$

Such that:

$$\begin{aligned} x(0) &= x_0 & y(0) &= y_0 \\ x(T) &= x_f & y(T) &= y_f \end{aligned} \quad (2.15)$$

We use direct methods in optimal control to solve the optimization problem. For this, we discretize the equations 2.10 to 2.13 into  $N$  discrete equations each corresponding to  $N$  time steps. We use forward differencing scheme, to generate the set of difference equations. For numerical reasons, we truncate the summation in equation 2.13 to finite number of terms. The difference equations obtained are as follows:

$$(1 + 2\pi_m)(\Omega[i+1] - \Omega[i]) = -4g(i)\Delta t + (1 + \pi_m)\pi_g \sin(\gamma[i])\Delta t \quad (2.16)$$

$$x(i+1) = x(i) + \Omega(i) \cos(\gamma(i))\Delta t \quad (2.17)$$

$$y(i+1) = y(i) - \Omega(i) \sin(\gamma(i)) \Delta t \quad (2.18)$$

$$g(i) = \sum_{j=1}^{i-1} \left( \sum_{k=1}^{n((i-j)\Delta t)} \exp(-\lambda_k^2(i-j)\Delta t) \right) (\Omega[j+1] - \Omega[j]) \quad (2.19)$$

The truncation limit  $n((i-j)\Delta t)$  is chosen such that the addition of an extra term would not change the value of the sum by more than a threshold value ( $\sim 10^{-14}$ ). Simplifying the above equations, we get the following:

$$(1+2\pi_m)(\Omega[i+1]-\Omega[i]) = -4 \sum_{j=1}^{i-1} (Coe f[i, j, \Delta t](\Omega[j+1]-\Omega[j])\Delta t) + (1+\pi_m)\pi_g \sin(\gamma[i])\Delta t \quad (2.20a)$$

$$Coe f[i, j, \Delta t] = \sum_{k=1}^{n[(i-j)\Delta t]} \exp(-\lambda_k^2(i-j)\Delta t) \quad (2.20b)$$

Equation 2.20 must be satisfied  $\forall i \in [1, N]$  while  $\Omega(1) = 0$ . The constraints on the terminal position of the cylinder obtained from equations 2.17 and 2.18 are as follows:

$$x_f = x_0 + \sum_{i=1}^N \Omega(i) \cos(\gamma(i)) \Delta t \quad (2.21)$$

$$y_f = y_0 - \sum_{i=1}^N \Omega(i) \sin(\gamma(i)) \Delta t \quad (2.22)$$

The resulting optimization problem becomes:

Minimize  $N \times \Delta t$  with equations 2.20, 2.21 and 2.22 as constraints.

### 3. Results

As discussed before, the deviation of a brachistochrone curve from cycloid is expected to be zero both at high and low viscosity ranges. There exists a particular  $\pi_g^*$  at which the deviation is maximum. The geometric deviation is defined as the following:

$$\delta = \int_{x_0}^{x_f} |y(x) - y_{cyc}(x)| dx \quad (3.1)$$

Where,

$\delta$  is the geometric deviation

$y(x)$  is the actual brachistochrone curve

$y_{cyc}(x)$  is the cycloid curve

The kinematic deviation is defined as the following:

$$T^* = \frac{T_{brac}}{T_{cyc}} \quad (3.2)$$

Where,

$T^*$  is the kinematic deviation

$T_{brac}$  is the total travel time of the fluid filled cylinder on the brachistochrone curve

$T_{cyc}$  is the time taken by a particle on a cycloid with same terminal point

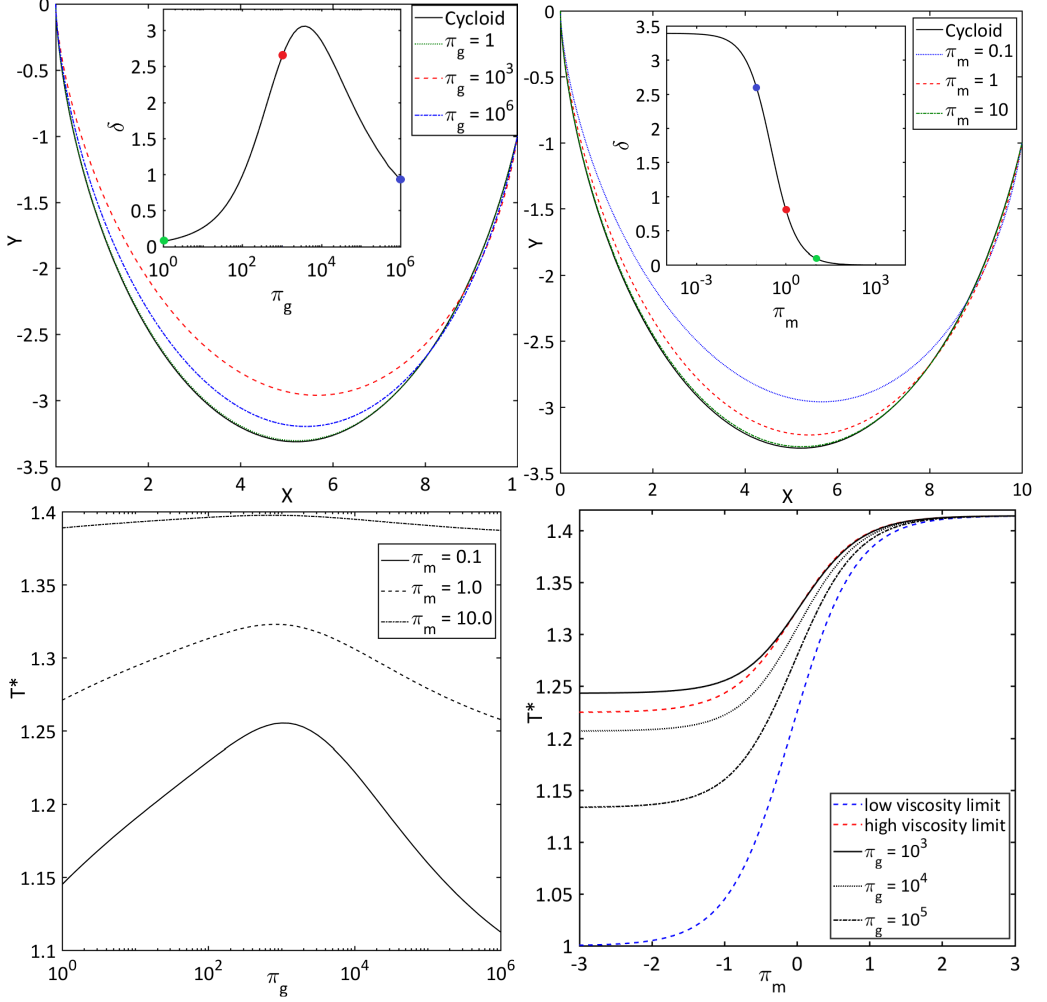


FIGURE 2. The figure shows the variation of brachistochrone curve with  $\pi_g$  at  $\pi_m = 0.1$  (top left) and with  $\pi_m$  at  $\pi_g = 1000$  (top right). The subplot inside each figure shows the geometric deviation  $\delta$  of the curve as a function of the parameters  $\pi_m$  and  $\pi_g$ . The kinematic deviation plotted against  $\pi_g$  and  $\pi_m$  are shown in the in the bottom left and bottom right respectively.

The variation of the geometric deviation ( $\delta$ ) with respect to  $\pi_g$  shows a peak as expected. For the terminal point at  $(10, -1)$  and  $\pi_m = 0.1$ , the peak occurs at  $\pi_g \approx 3981$ . The variation of the geometric deviation with respect to  $\pi_m$  shows a sigmoid-like behavior with an inflection point at  $\pi_m \approx 1$ . At low viscosity limit, the fluid filled cylinder is effectively a hoop with mass  $M$  and a point mass with mass  $m$  at the center. Where as, at high viscosity limit, the fluid filled cylinder acts like a solid cylinder with the mass of the fluid and a hoop with the mass of the solid cylinder. So, at these two limits, dynamics of the fluid filled cylinder will boil down to rigid body dynamics which is the reason for the geometric deviation  $\delta$  to vanish at the high and low limits of viscosity. Also, at both low and high viscosity cases, the dissipation due to the fluid vanishes. The reasons being low viscosity coefficient and absence of velocity gradients respectively. This means that at both these limits, fluid filled cylinder will be faster than at other viscosity values. This fact can be verified from the plot on the bottom left figure 2. As the mass of fluid

decreases i.e.,  $\pi_m$  increases, the effect of fluid will diminish leaving only the cylindrical shell. This is illustrated in the plot on the bottom left of figure 2 by the fact that the plot of kinematic deviation ( $T^*$ ) against  $\pi_g$  is becoming flatter at higher  $\pi_m$  values. The asymptotic value of  $T^*$  is square root of the ratio of the net inertial mass of a hoop to that of a particle. This turns out to be  $\sqrt{2}$ . Convergence to this limit is clearly seen in the bottom left plot of figure 2.

#### 4. Stability of fluid flow

The previous section discussed the properties of a fluid filled cylinder performing a brachistochrone motion. All the while, we assume that flow field is governed by equation 2.8 and the viscous torque due to the fluid flow is as mentioned in 2.17. We now question this assumption and check for stability of the assumed flow field.

##### 4.1. Linear stability equations

On linearizing the navier-stokes equations in polar coordinates and simplifying them with axisymmetric assumption and normal mode assumption of  $f(r, \theta, z, t) = \hat{f}(r, t) \exp(kz)$ , we obtain the following equations:

$$(DD^* - \alpha^2 - \frac{1}{\nu} \frac{\partial}{\partial t}) \hat{\psi} = \frac{2\alpha^2 V_b \hat{v}}{\nu r} \quad (4.1)$$

$$(DD^* - \alpha^2) \hat{u} = \hat{\psi} \quad (4.2)$$

$$(DD^* - \alpha^2 - \frac{1}{\nu} \frac{\partial}{\partial t}) \hat{v} = \frac{\hat{u} D^* V_b}{\nu} \quad (4.3)$$

Where,

$$D = \frac{\partial}{\partial r}$$

$$D^* = D + \frac{1}{r}$$

The equations 4.1 to 4.3 are scaled by using the using the same scaling law used before.

$$(DD^* - k^2 - \frac{\partial}{\partial t}) \hat{\psi} = \frac{2k^2 V_b \hat{v}}{r} \quad (4.4)$$

$$(DD^* - k^2) \hat{u} = \hat{\psi} \quad (4.5)$$

$$(DD^* - k^2 - \frac{\partial}{\partial t}) \hat{v} = \hat{u} D^* V_b \quad (4.6)$$

The boundary conditions for 4.4 to 4.6 are as follows:

$$\left. \begin{aligned} \hat{u}(1, t) &= \hat{v}(1, t) = D^* \hat{u}(1, t) = 0 \\ \hat{u}(0, t) &= \hat{v}(0, t) = D^* \hat{u}(0, t) = 0 \\ \hat{\psi}(1, t) &= \frac{\partial^2 \hat{u}}{\partial r^2}(1, t) \\ \hat{\psi}(0, t) &= \frac{\partial^2 \hat{u}}{\partial r^2}(0, t) \end{aligned} \right\} \quad (4.7)$$

##### 4.2. Solution to the linear stability equations

To solve for the linear stability equations 4.4 to 4.7 and comment on the stability of the fluid flow, we adopt the same methodology used by [Chen & Kirchner \(1971\)](#)

with slight modifications. The idea is to give an initial perturbation to the time varying flow and let it decay as long as the flow is stable. When the flow becomes unstable, the perturbation starts to grow. The instant when the growth begins is the point of instability. For numerical reasons, we spike the perturbation energy whenever it falls below a threshold. This is done so that the perturbation energy doesn't decay to a value lower than machine precision. We discretize the equations 4.4 to 4.7 using finite difference method and solve the resulting system of linear equations. The following are the obtained discrete equations:

$$\hat{u}^{k+1}(n, j) = \frac{\omega}{\lambda_j} (\alpha_j \hat{u}^k(n, j+1) + \beta_j \hat{u}^{k+1}(n, j-1) - (\Delta r)^2 \Psi(n, j)) - (\omega - 1) \hat{u}^k(n, j) \quad (4.8)$$

$$\Psi(n+1, j) = \Psi(n, j) + \frac{\Delta t}{(\Delta r)^2} \left( \alpha_j \Psi(n, j+1) + \beta_j \Psi(n, j-1) - \lambda_j \Psi(n, j) + \frac{2k^2 V_b(n, j) \hat{v}(n, j) (\Delta r)^2}{r_j} \right) \quad (4.9)$$

$$\hat{v}(n+1, j) = \hat{v}(n, j) + \frac{\Delta t}{(\Delta r)^2} \left( \alpha_j \hat{v}(n, j+1) + \beta_j \hat{v}(n, j-1) - \lambda_j \hat{v}(n, j) + \frac{\hat{u}(n, j) \Delta r}{2} (V_b(n, j+1) - V_b(n, j-1) + \frac{2\Delta r}{r_j} V_b(n, j)) \right) \quad (4.10)$$

The perturbation energy is given by:

$$E_p = \pi \int_1^R r \left[ u^2 + v^2 + \frac{1}{k^2} (D^* u)^2 \right] dr \quad (4.11)$$

#### 4.3. Linear stability for the case of a brachistochrone fluid filled cylinder

Intuition tells us that if the terminal point of the brachistochrone curve is farther below the initial point, the flow is likely to become unstable even before it reaches the terminal point. Whereas, if the terminal point is vertically closer to the initial point, the flow is likely to remain stable till it reaches the terminal point. So, there would exist a boundary separating terminal points with completely stable fluid flow and those which will lead to an instability before reaching the terminal point. The following exercise is an attempt at capturing this boundary. The figure 3 shows this exercise of finding the stable and unstable terminal points.

Clearly from the figure 3 the plot on the right top is stable because there is no point at which the perturbation energy grows whereas the plot on the right bottom shows exponential growth in perturbation energy. So, this brachistochrone curve would be marked as unstable. The left plot shows that the stable region expands as the horizontal separation between the terminal and initial points increases. This is explained by the flattening of the brachistochrone curves at these cases.



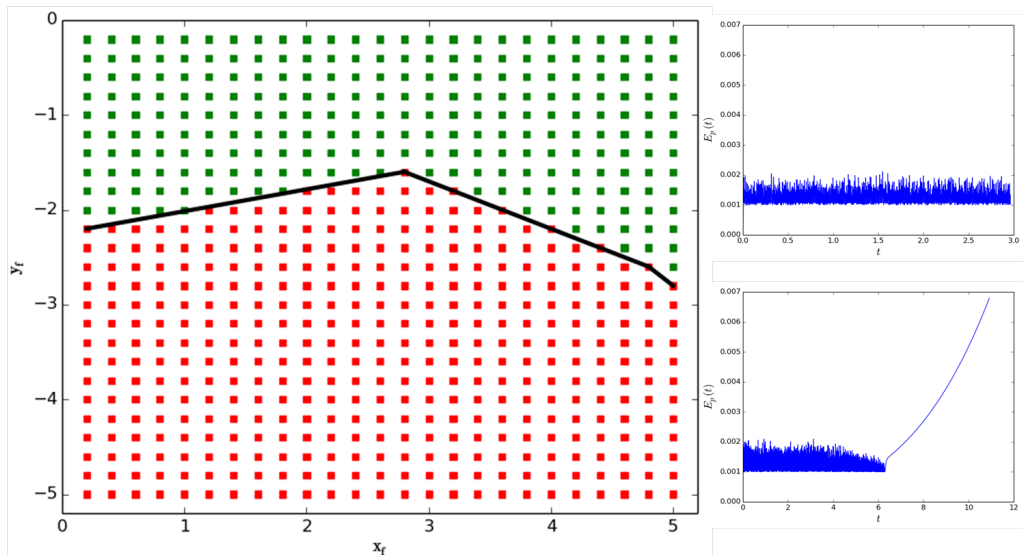


FIGURE 3. The figure shows the stable (in green) and unstable (in red) terminal points and the approximate stability margin (in black) for  $\pi_m = 0.1$  and  $\pi_g = 0.1$ . For every case, the first occurrence of instability is at  $k \rightarrow 0$ . The plot on the top right shows the perturbation energy of a stable brachistochrone curve ( $x_f = 0.2$ ,  $y_f = -0.2$ ) and the plot on the bottom right shows that for an unstable brachistochrone curve ( $x_f = 0.2$ ,  $y_f = -5.0$ ) both at  $\pi_m = 0.1$  and  $\pi_g = 0.1$

## 5. Discussion

By analyzing the stability of brachistochrone curves for different  $\pi_m$  and  $\pi_g$ , we understand that for higher values of  $\pi_g$  the stable region shrinks. We see that for an Aluminum ( $\rho = 2700 \text{ kg/m}^3$ ) beverage can of radius 3 cm, height 10 cm and thickness 0.5 mm filled with silicone oil ( $\rho = 975 \text{ kg/m}^3$ ) of viscosity 5000 cSt, the non-dimensional quantities  $\pi_m$  and  $\pi_g$  are approximately equal to 0.1 and 10 respectively. The brachistochrone curve for this Aluminum can with end points at  $x = 30$  cm and  $y = -3$  cm will deviate significantly from the classic cycloid with the laminar flow inside it being stable.

## REFERENCES

- ANDRE-SOHN, E. 1696 *Acta Eruditorum: Anno ... publicata. 1696*. Georgius.
- BACHELOR, G. K. 2000 *An Introduction to Fluid Dynamics*. Cambridge University Press.
- CHEN, C. F. & KIRCHNER, R. P. 1971 Stability of time-dependent rotational couette flow part 2. stability analysis. *Journal of Fluid Mechanics* **48** (2), 365384.
- GEMMER, J., UMBLE, R. & NOLAN, M. 2006 Generalizations of the Brachistochrone Problem. *ArXiv Mathematical Physics e-prints*, arXiv: math-ph/0612052.
- LIBERZON, DANIEL 2011 *Calculus of Variations and Optimal Control Theory: A Concise Introduction*. Princeton, NJ, USA: Princeton University Press.
- LIPP, STEPHEN C. 1997 Brachistochrone with coulomb friction. *SIAM Journal on Control and Optimization* **35** (2), 562–584, arXiv: <https://doi.org/10.1137/S0363012995287957>.
- SUPEKAR, ROHIT B & PANCHAGNULA, MAHESH V 2014 Dynamics and stability of a fluid filled cylinder rolling on an inclined plane. *arXiv preprint arXiv:1408.6654*.
- VRATANAR, B. & SAJE, M. 1998 On the analytical solution of the brachistochrone problem in a non-conservative field. *International Journal of Non-Linear Mechanics* **33** (3), 489 – 505.